

Discontinuous Galerkin Spectral Element Approximations for CFD

D.A. Kopriva*
Florida State University
Tallahassee, FL 32306

G.B. Jacobs†
San Diego State University
San Diego, CA 92182

September 30, 2011

1 Code description

1.1 Discretization

The discontinuous Galerkin approximation generates a framework for developing solvers for conservation laws of the form

$$\begin{aligned}\vec{q}_t + \nabla \cdot \vec{f} &= 0 \\ \vec{f} &= \vec{f}^i + \vec{f}^v\end{aligned}$$

such as the Euler Equations of gas-dynamics

$$\vec{q} = \begin{bmatrix} \rho \\ \rho \vec{u} \\ \rho E \end{bmatrix}, \quad \vec{f}^i = \begin{bmatrix} \rho \vec{u} \\ \rho \vec{u} \otimes \vec{u} + pI \\ \rho uH \end{bmatrix}, \quad \vec{f}^v = 0$$

and the compressible Navier-Stokes Equations

$$\vec{f}^v = \begin{bmatrix} 0 \\ -\tau \\ \tau \cdot \vec{u} + k\nabla T \end{bmatrix}$$

The three basic characteristics are:

- Approximate the solution and fluxes by polynomials within elements

$$\tilde{q} \approx \tilde{Q} \in \mathbb{P}^N, \quad \tilde{f} \approx \tilde{F} \in \mathbb{P}^M \text{ on } E$$

*Professor, Department of Mathematics

†Associate Professor, Department of Aerospace Engineering

- Start with a weak form for the equations

$$\int_E (Q_t + \nabla \cdot F) \phi = 0$$

- and require no continuity on $\phi \in \mathbb{P}^N$ between elements.

1.2 Relevant solvers

Within these broad constraints one has a huge number of choices:

1. Use Quad/Hex or Tri/Tet elements?
2. Use a Nodal or a modal basis?
3. What basis polynomials?
4. Approximate boundaries with different orders?
5. Approximate solution and fluxes with different orders?
6. Exact integrals or quadrature?
7. Inexact or exact quadrature?
8. Integrate by parts once or twice?
9. ...

We will present solutions to the workshop benchmark problems using a “Classical” spectral element approximation:

- Quadrilateral/ Hexahedral elements for efficient tensor product bases
- A Nodal basis for Easy for nonlinear/variable coefficient/general complex geometry problems.
- All approximations at same polynomial order, which Simplifies coding
- Legendre Polynomial basis for spectral accuracy and p -refinement
- Legendre-Gauss quadrature
- Isoparametric element boundaries

These choices lead to a spectrally accurate, unstructured mesh approximation that is nevertheless simple to code. Within each element one updates the solution by

$$\begin{aligned} \frac{d\mathbf{Q}_{i,j}}{dt} + \left\{ \left[\tilde{\mathbf{F}}^*(1, \eta_j) \frac{\ell_i(1)}{w_i^{(\xi)}} - \tilde{\mathbf{F}}^*(-1, \eta_j) \frac{\ell_i(-1)}{w_i^{(\xi)}} \right] + \sum_{k=0}^N \tilde{\mathbf{F}}_{k,j} \hat{D}_{ik}^{(\xi)} \right\} \\ + \left\{ \left[\tilde{\mathbf{G}}^*(\xi_i, 1) \frac{\ell_j(1)}{w_j^{(\eta)}} - \tilde{\mathbf{G}}^*(\xi_i, -1) \frac{\ell_j(-1)}{w_j^{(\eta)}} \right] + \sum_{k=0}^N \tilde{\mathbf{G}}_{i,k} \hat{D}_{jk}^{(\eta)} \right\} = 0, \end{aligned}$$

where $\tilde{\mathbf{F}}^*$ represents the Riemann Flux.

Time integrators include explicit Runge-Kutta, orders one to four, including low dissipation and dispersion error versions, Implicit Runge-Kutta up to order four and BDF up to order four with Newton-Raphson with GMRES or BICGSTAB linear solvers.

1.3 High-order capability

Any order depending on polynomial order approximation, N , within element. Spectrally accurate.

1.4 Parallel capability

Full parallel capability, tested on 10k processors.

1.5 Post-processing

Turbulence statistics. Tecplot, Matlab, Fieldview

1.6 Other features used for case (e.g. adaptivity)

Non-conformal, adaptive grid, using mortar approach.

2 Case summary

We solve the flat plate, bump flow and NACA0012 problems posed in the workshop case directory. We will determine the residual tolerances and other convergence criteria that were requested on parallel machines at Florida State University and San Diego State University.

2.1 Meshes

Meshes were created with an in-house mesher with high-order (isoparametric) boundary fitting. The mesh for the NACA test problems are shown in Figures 1 and 2. The mesh used for the flat plate computation is shown in Figure 5a.

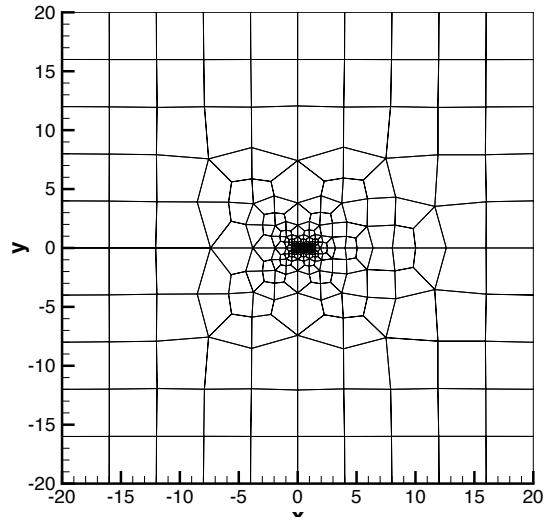


Figure 1: The mesh for $M = 0.5$ flow over a NACA0012 airfoil at 2deg. angle of attack.

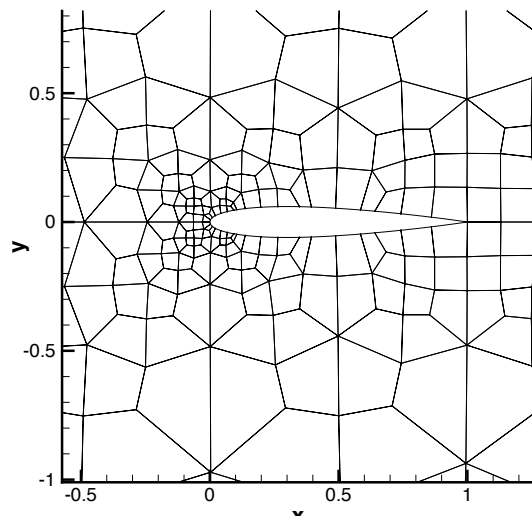


Figure 2: The mesh in the neighborhood of the airfoil for $M = 0.5$ flow over a NACA0012 airfoil at 2deg. angle of attack.

3 Results

3.1 Problem C.1.1: Inviscid Flow over a Bump in a Channel

Fig. 3 shows pressure contours for the $M=0.5$ inviscid flow over a smooth bump in a channel using the DGSEM and fifth order polynomial approximations.

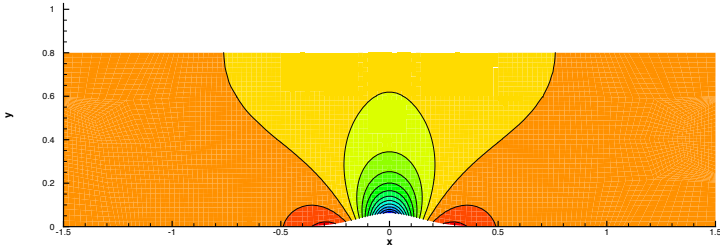


Figure 3: Pressure contours for a fifth order polynomial approximation to flow over a smooth bump.

3.2 Problem C.1.3: Flow over a NACA0012 Airfoil

The DGSEM is geometrically flexible. In Fig. 4 we show $N = 5$ order solutions to the $M = 0.5$ flow over a NACA0012 airfoil at 2 deg angle of attack.

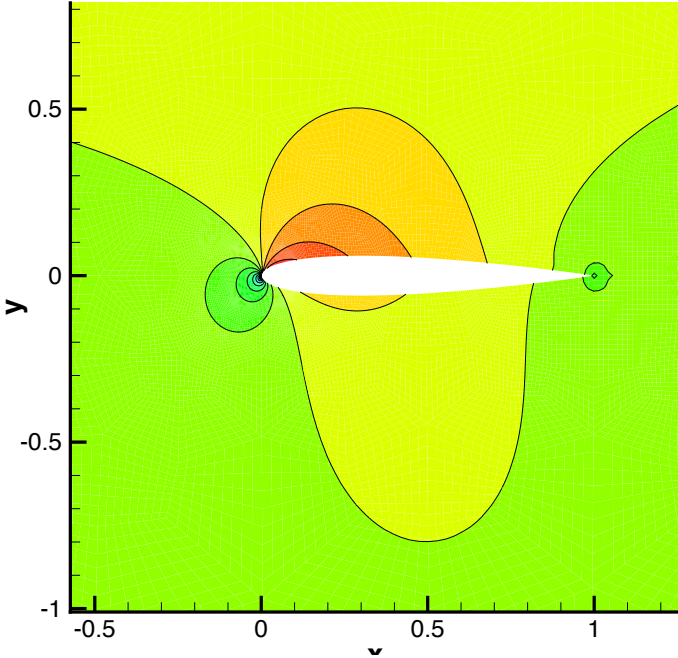


Figure 4: Mach contours for $M = 0.5$ flow over a NACA0012 airfoil at 2deg. angle of attack.

3.3 Problem C.1.4: Flat Plate Boundary Layer

The DGSEM is also applicable to viscous compressible problems. Fig. 5 shows a flat plate computation of the type requested at $M = 0.6$ and $RE = 1000$. A different mesh would be used for the requested $RE = 10^6$ computation. Fig. 5 compares the horizontal velocity profile as a function of height from the plate at $x = 12$.

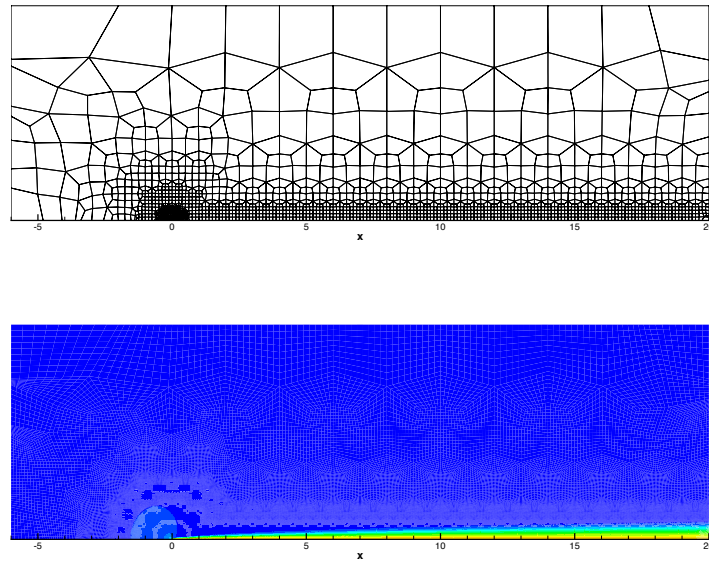


Figure 5: Mesh and temperature contours for flow over a flat plate

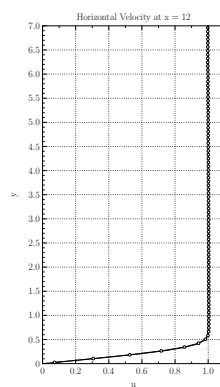


Figure 6: Horizontal velocity for the boundary layer flow at $x = 12$